FOLIA HISTOCHEMICA ET CYTOBIOLOGICA
Vol. 62, No. 2, 2024
pp. 87–98

ORIGINAL PAPER

VIA MEDICA

Simvastatin suppresses ethanol effects on the kidney of adolescent mice

Makgotso Nchodu, Robin du Preez, Alice Efuntayo, Oladiran I Olateju

School of Anatomical Sciences, Faculty of Health Sciences, University of the Witwatersrand, Johannesburg, South Africa

Abstract

Introduction. Adolescents tend to experiment with ethanol which often results in heavy episodic drinking patterns leading to serious health concerns later in life. Chronic ethanol use damages renal tissue, promotes collagen deposition, and induces renal inflammation, thereby causing renal dysfunction. Therefore, an intervention such as simvastatin (a blood cholesterol-lowering drug) that could suppress the effects of ethanol on the kidney may be beneficial. This study explored the impact of simvastatin against the onset of renal morphological damage, fibrosis, and inflammation caused by ethanol exposure in mice.

Materials and methods. Ten four-week old C57BL/6J mice (F = 5; M = 5) were assigned to each experimental group: (I) NT; no administration of ethanol or simvastatin; (II) EtOH; 2.5 g/kg/day of 20% ethanol, intraperitoneal injection (*i.p.*); (III) SIM; 5 mg/kg/day of simvastatin, orally; (IV) EtOH + SIM5; 5 mg/kg/day of simvastatin, orally, followed by 2.5 g/kg/day of 20% ethanol, *i.p.*; and (V) EtOH + SIM15; 15 mg/kg/day of simvastatin, orally, followed by 2.5 g/kg/day of 20% ethanol, *i.p.* After the 28-day treatment period, the right kidney was removed and processed for haematoxylin and eosin staining, Masson's trichrome staining, or tumour necrosis factor-alpha (TNF-α) immunohistochemistry. The renal corpuscular area, glomerular area, and urinary space area were measured and the area of collagen or TNF-α expression was quantified using ImageJ software.

Results. Ethanol administration significantly increased the renal corpuscular area, the glomerular area, the area of collagen, and the area of tissue with TNF-α immunoreactivity but decreased the area of urinary space. Simvastatin generally suppressed the ethanol effects in both sexes, although to varying degrees.

Conclusions. Simvastatin proved to suppress collagen deposition and the TNF-α production induced by ethanol in the kidney of mice thus indicating its effectiveness in the treatment of ethanol-related renal diseases. (*Folia Histochem Cytobiol 2024; 62, 2: 87–95*)

Keywords: ethanol; kidney; simvastatin; fibrosis; TNF-alpha; sex effect

INTRODUCTION

Apart from the regulation of body fluid and mineral homeostasis, the kidneys play an important role in the control of blood pressure [1]. They are also responsible for filtering and excreting ethanol and its metabolites from the body [2], making the kidneys highly vulnerable to damage caused by excessive ethanol consumption [3]. Due to the function of the kidneys, damage or loss of function could negatively affect the functions of other organs, especially the heart [4]. It is proven that chronic consumption of ethanol increases the incidence of cardiovascular diseases [5, 6] by increasing blood pressure through various mechanisms, one of which is the activation of the renin-angiotensin system (RAS) in the kidney where a rise in systemic blood pressure causes glomerular hypertension and vasoconstriction [1]. The activated intrarenal RAS induced by chronic ethanol use also promotes renal damage by altering the morphologies of the glomeruli, tubules, and renal blood vessels [1, 7, 8]. Simultaneously, it prolongs hypertension

Correspondence address:
Oladiran I. Olateju
School of Anatomical Sciences, Faculty of Health Sciences, University of the Witwatersrand, 7 York Road, Parktown, 2193, Johannesburg, Republic of South Africa
tel. +27 11 717 2763; fax: +27 11 717 2422
e-mail: Oladiran.Olateju@wits.ac.za

This article is available in open access under Creative Common Attribution-Non-Commercial-No Derivatives 4.0 International (CC BY-NC-ND 4.0) license, allowing to download articles and share them with others as long as they credit the authors and the publisher, but without permission to change them in any way or use them commercially.

©Polish Society for Histochemistry and Cytochemistry
Folia Histochem Cytobiol. 2024
DOI: 10.5603/fhc.95685
ISSN 0239-8508, e-ISSN 1897-5631

www.journals.viamedica.pl/folia_histochemica_cytobiologica

which is detrimental to the heart and other organs [1, 9]. This interrelationship between the heart and the kidneys shows that the severity of cardiovascular disease increases the probability of renal disease and *vice versa* [8]. Unfortunately, chronic ethanol consumption is a social problem among adolescents as they tend to experiment with ethanol, often resulting in heavy episodic drinking patterns, especially in places where there are lapses in the regulation of access to ethanol [10–12]. Ethanol misuse is higher in male than in female adolescents and these adolescents often become ethanol addicts later in life thus contributing to social, economic, and health problems [5, 11–15].

Ethanol-induced renal damage changes the morphologies of the renal structures, *e.g.* the glomeruli and renal tubules. This causes renal functions such as glomerular filtration and tubular reabsorption to fail [2, 4, 7, 16, 17]. At the same time, chronic ethanol use inhibits the function of antidiuretic hormone (ADH) in the kidneys thus resulting in the loss of water from the body [17]. Likewise, extracellular matrix deposition (*i.e.* renal fibrosis) between the renal tubules and surrounding capillaries may increase in response to chronic ethanol use, delaying the oxygen supply and nutrients to the renal tubular cells [2].

Tumour necrosis factor-alpha (TNF-α) is produced in the kidney by endothelial, mesangial, and renal tubular epithelial cells [9, 18]. The basal interstitial level of TNF-α is considerably low or undetectable under normal conditions but it sporadically increases at the onset of inflammation. TNF-α can also induce apoptosis which may be beneficial or detrimental to renal tissues as apoptosis may contribute to the pathogenesis of renal diseases such as acute renal failure or may trigger cell proliferation to compensate for glomerular or tubular cell loss in glomerular or tubular disease [19].

With the plethora of effects of simvastatin on the cardiovascular system, it is envisaged that the ability of simvastatin (an FDA-approved blood cholesterol-lowering drug [20–23]) to prevent inflammation, regulate immune-responses, prevent cell death and fibrosis in diseases associated with a failing cardiovascular system [24–27] may also be of benefit against ethanol-induced renal damage. This study, therefore, explored the effects of simvastatin against ethanol-induced renal damage, fibrosis, or inflammation by analysing the morphology and morphometry of renal structures, quantifying the area of collagen and the area of TNF-α expression in the renal tissue of adolescent mice that were administered ethanol. Results of this study may provide new cues on the protective effects of simvastatin against ethanol-induced damage in the kidneys and may also provide additional evidence of its suitability for the treatment of alcohol-related renal diseases.

MATERIALS AND METHODS

Animals and study design

Animal ethics approval was granted (Ethics Clearance No: 2019/11/63/C) by the Animal Research Ethics Committee (AREC) of the University of the Witwatersrand, Johannesburg, South Africa. Mice of the same sex and belonging to the same experimental group were housed together in a group of five mice per cage (cage dimensions: 200 × 200 × 300 mm) and kept under a reversed 12-hour day/12-hour dark cycle (with the light switched off from 06:00 to 18:00). For this study, the period of adolescence in the mice was taken as between 3–8 weeks old [28].

Ten four-week old (adolescent) C57BL/6J mice (F = 5; M = 5) housed in the Witwatersrand Research Animal Facility (WRAF), University of the Witwatersrand, were assigned to each experimental group: (I) non-treatment group (NT) — no administration of ethanol or simvastatin; (II) Ethanol only group (EtOH) — 2.5 g/kg/day of 20% ethanol *via* intraperitoneal injection (*i.p.*); (III) simvastatin only group (SIM) — 5 mg/kg/day by oral gavage; (IV) ethanol and 5 mg simvastatin (EtOH + SIM5) — 5 mg/kg/day of simvastatin by oral gavage followed by 2.5 g/kg/day of 20% ethanol *via i.p.* administration; (V) ethanol + 15 mg simvastatin (EtOH + SIM15) — 15 mg/kg/day of simvastatin by oral gavage followed by 2.5 g/kg/day of 20% ethanol *via i.p.* administration. The percentage concentration of ethanol used in this study was similar to the range used by Cardoso de Sousa *et al.* [29]. An intraperitoneal injection of ethanol is commonly used in ethanol-related studies to generate a high blood ethanol concentration (see review by Patten *et al.* [30]). In addition, the concentrations of simvastatin used were also within the range used by Mohammadi *et al.* [31]. A stock solution of simvastatin (Cat no: 1612700, Merck, South Africa) was prepared by dissolving 8 mg simvastatin in a solution of 100 μL ethanol (to increase solubility), 100 μL 0.1 M NaOH (emulsifier) and 800 μL distilled water similarly as described by McKay *et al.* [32]. In addition, a pharmacological grade ethanol (96%) (Sigma-Aldrich, South Africa; Cat no: SAAR-2233510LP) was serially diluted in saline (0.9% NaCl) to obtain a 20% ethanol solution. Both simvastatin and ethanol were prepared daily and then filter sterilized before being administered. Any unused solution on the day was discarded. All treatments were performed for 28 consecutive days. Oral gavage and intraperitoneal injections were performed with the utmost care by the trained staff of WRAF to reduce the introduction of stress into the animal.

On the last day of treatment, blood alcohol concentration (BAC) was determined from saphenous blood (50 μL) collected within 30 min after the administra-

©Polish Society for Histochemistry and Cytochemistry
Folia Histochem Cytobiol. 2024
DOI: 10.5603/fhc.95685
ISSN 0239-8508, e-ISSN 1897-5631

tion of ethanol in each mouse (*i.e.* mice in the ETOH, ETOH + SIM5 or ETOH + SIM15 experimental groups). The BAC in the extracted serum was analysed using an EnzyChrom™ Ethanol Assay Kit (BioVision, Sandton, South Africa). The average BAC level was in the range of 182.5–253.4 mg/dL for the groups that received ethanol. Following blood collection, the mice were euthanized using Euthanaze (sodium pentobarbital, 80 mg/kg, *i.p.*). Then, the mice were transcardially perfused with 20 mL 4% paraformaldehyde (PFA) (in 0.1 M phosphate buffer, PB), the right kidney was then removed and further fixed in 4% buffered PFA at 4°C before further processing.

Processing of the kidney

The kidney was cut horizontally at its equator whereafter the inferior half of the tissue was dehydrated in a graded series of ethanol, cleared in xylene, and then embedded in paraffin wax. The tissue block was sectioned at 5 μm thickness and one in three series of sections was collected for haematoxylin and eosin (H&E) staining (for general morphology and morphometry of renal corpuscles and the glomeruli). The second series of sections was prepared for Masson's trichrome (MT) staining (for evaluating the area of collagen) and the third series of sections was for TNF-α immunohistochemistry (for quantifying the area of TNF-α expression in the renal corpuscles or renal tubules). In total, four sets of one in three series of sections were collected. A 50 μm-thick section was wasted after each set of series to minimize analysing the same area of the section.

Immunohistochemistry

For TNF-α immunohistochemistry, a citrate antigen retrieval was performed by immersing the sections in citrate buffer (pH 6) at 60°C overnight. Thereafter, endogenous peroxidase activity was blocked by immersing the sections in 1% hydrogen peroxide, 49.5% methanol and 49.5% 0.1 M PB for 30 min. Subsequently, the sections were washed twice in 0.1 M PB before incubating in a blocking buffer (5% normal goat serum in 0.1 M PB) for 30 min to block unspecified binding sites. Thereafter, the sections were incubated overnight at 4°C in the primary antibody (1:250, mouse anti-TNF-α, ab220210, Abcam, Cambridge, United Kingdom) to quantify the area of tissue that expressed TNF-α immunoreactivity (TNFα-IR) The sections were then washed twice in 0.1 M phosphate-buffered saline before incubating in the secondary antibody (1:1000, goat anti-mouse IgG, BA-9200-1.5, Vector labs). Following incubation, the sections were washed twice in PB before incubating in an avidin-biotin solution (1:125; Vector Labs) for 1 h. The sections were further washed twice in PB and then the sections were developed by immersing them in a solution containing 0.05% DAB (3,3'-diaminobenzidine), 2 mL Tris HCl, 29 μL cold distilled water, and 1 μL hydrogen peroxide for 10 mins. The DAB reaction was terminated by adding an equal volume of 0.1 M PB before counterstaining with haematoxylin.

Histomorphometry

For the morphometry of renal structures, the renal corpuscles that were visible within a field of view at the 10× objective lens (obtained by moving the stage at every 1-mm interval along the width of the renal cortex of H&E-stained sections) were used for the morphometry. Each renal corpuscle within this field of view was then photographed at the 63× objective lens using a Carl Zeiss Axiocam camera (Serial No. 5318003446, Shanghai, China) attached to a Carl Zeiss Axioskop microscope (Serial No. 804161, Germany). With the scale set on ImageJ 1.47v software (NIH, Bethesda, MD, USA), the areas of the renal corpuscle and the glomerulus were measured from the digitized images by tracing the boundary of the parietal layer of the Bowman's capsule and the boundary of the glomerulus using the freehand tool of the software. The area of Bowman's space was then calculated by subtracting the area of the glomerulus from the area of the renal corpuscle [33].

To determine the area of collagen in the kidney tissue, digitized images of the MT-stained sections were taken using a Carl Zeiss Axiocam camera attached to a Carl Zeiss Axioskop microscope at times 40× objective lens. The images were subsequently saved in a JPEG file format. The field of view was changed by moving the microscope stage along the width of the renal cortex to prevent duplicating measurements. The area of stained collagen within the kidney was determined using the deconvolution plugin settings of ImageJ software [34, 35]. The 24-bit RGB format was selected as a requirement for the deconvolution plugin setting in the software where the green component on the processed image indicated collagen staining [34, 35]. The area of stained collagen on each image was quantified using the threshold tool on the software which was adjusted until all the collagen (*i.e.* green-stainable) structures had been highlighted [34, 35]. The percentage area of collagen *per* image was calculated as the threshold area divided by the area of the image.

Similar to the analyses used for MT-stained sections, the percentage area of tissue with TNFα-IR in the renal tubules or the renal corpuscles was performed using digitized images at the 63× objective lens. The renal tubules or renal corpuscles were identified and photographed along the width of the renal cortex to prevent duplicating measurements. The digitized

©Polish Society for Histochemistry and Cytochemistry

DOI: 10.5603/fhc.95685
ISSN 0239-8508, e-ISSN 1897-5631

images were saved in a JPEG file format before being analysed by ImageJ software. Using the 24-bit RGB format, the region of interest (ROI) manager was used to select the renal corpuscle or the renal tubules on an image. The size of the ROI (620368 μm^2) was kept constant throughout the analyses [36]. DAB staining was selected for the deconvolution plugin setting on the ImageJ software where the brown component was identified as the DAB staining. The area of tissue that expressed TNF-α in each ROI was quantified by adjusting the threshold tool of the software until all the DAB stains had been highlighted [36]. Thereafter, the percentage area of tissue with TNFα-IR was determined by dividing the threshold area by the area of the ROI. Throughout the analyses, the experimenter was blinded to the experimental groups and an inter-observer test was satisfactory.

Statistical analysis

Descriptive statistics using the mean and standard deviation (SD), or the median were performed. Normality test was conducted using the Shapiro-Wilk test and then either One-Way ANOVA or Kruskal-Wallis test was conducted to compare the mean or median of the measurements across the different groups. A *post hoc* test using either a Tukey's or a Dunn's test was conducted to determine where significant difference lies between any two groups. All statistical tests were performed using a PAST freeware data analyser (version 4.03; Germany) and boxplots were plotted using Excel software (Word Office Pro, Redmond, WA, USA). A statistical difference of 5% was regarded as significant for all statistical analyses ($P < 0.05$).

RESULTS

Kidney and body mass and morphology of the kidney

The average kidney mass, body mass and kidney/body mass ratio of the mice across the different experimental groups for both sexes are shown in Table 1. The average kidney mass, the average body mass or the kidney/body mass ratio was similar across the experimental groups for both sexes. In addition, all the mice in the different experimental groups gained body mass, for both sexes.

The morphology of the tissue was typical of the normal histology of the renal tissue of the mouse. The renal corpuscles and the renal tubules were distinct and abundant in the renal cortex across the different

Table 1. Mean kidney mass, mean body mass and kidney/body mass ratio of female and male mice across the experimental groups

	NT	SIM	EtOH	EtOH + SIM5	EtOH + SIM15	P
Female						
Kidney mass at day 28 [g]	0.162 ± 0.013	0.151 ± 0.028	0.169 ± 0.017	0.149 ± 0.039	0.183 ± 0.015	0.203
Body mass at day 1 [g]	12.500 ± 0.791	12.800 ± 0.758	12.600 ± 0.822	12.000 ± 0.935	12.700 ± 0.274	0.652
Kidney/body mass ratio at day 1	0.014 ± 0.001	0.012 ± 0.002	0.013 ± 0.001	0.012 ± 0.004	0.014 ± 0.001	0.311
Body mass at day 28 [g]	14.500 ± 1.581	14.800 ± 1.151	14.600 ± 1.245	13.900 ± 1.025	15.300 ± 1.891	0.639
Kidney/body mass ratio at day 28	0.012 ± 0.001	0.010 ± 0.003	0.012 ± 0.002	0.010 ± 0.003	0.012 ± 0.001	0.493
Male						
Kidney mass at day 28 [g]	0.162 ± 0.016	0.158 ± 0.010	0.177 ± 0.014	0.181 ± 0.016	0.177 ± 0.031	0.240
Body mass at day 1 [g]	15.300 ± 0.975	14.300 ± 1.304	14.400 ± 2.162	14.400 ± 0.742	13.700 ± 1.255	0.330
Kidney/body mass ratio at day 1	0.011 ± 0.002	0.012 ± 0.001	0.013 ± 0.003	0.013 ± 0.001	0.013 ± 0.003	0.438
Body mass at day 28 [g]	18.900 ± 1.673	18.400 ± 1.636	18.000 ± 1.658	18.100 ± 0.548	15.900 ± 1.387	0.072
Kidney/body mass ratio at day 28	0.009 ± 0.001	0.010 ± 0.002	0.010 ± 0.001	0.010 ± 0.001	0.011 ± 0.002	0.149

The values express mean ± SD (standard deviation). P indicates statistical difference (at 0.05) using One-Way ANOVA (parametric) or Kruskal-Wallis (non-parametric). There was no significant difference for all the measurements across the experimental groups. Abbreviations: NT — non-treatment (control) groups; SIM — 5 mg simvastatin; EtOH — ethanol; EtOH + SIM5 — 5 mg simvastatin and EtOH; EtOH + SIM15 — 15 mg simvastatin and EtOH.

©Polish Society for Histochemistry and Cytochemistry

DOI: 10.5603/fhc.95685
ISSN 0239-8508, e-ISSN 1897-5631

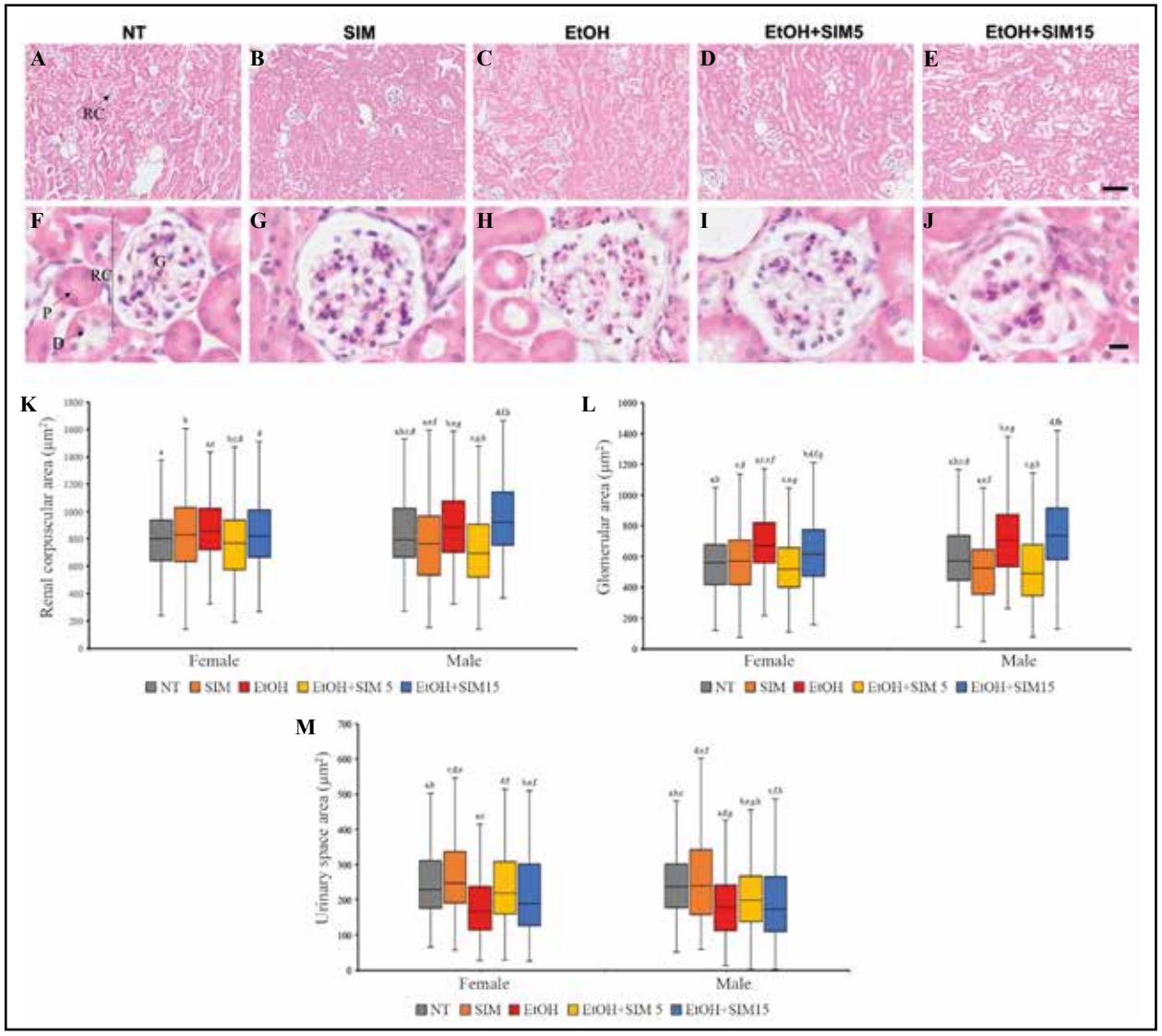

Figure 1. Representative photomicrographs of the H&E-stained sections of female and male mouse kidneys (**A–E**) at the low magnification (scale bar: 100 μm) and (**F–J**) at the high magnification (scale bar: 10 μm) as well as the box plots of the median values of: (**K**) kidney corpuscular area, (**L**) glomerular area, and (**M**) urinary space area across the different experimental groups. The renal morphology was typical of the normal histology of the mouse kidney with the renal corpuscles (RC), glomeruli (G), distal (D) and proximal (P) kidney tubules present in the renal cortex. In both sexes, ethanol increased the renal corpuscular and glomerular areas but decreased the urinary space area in the renal tissue. In both sexes, 5 mg simvastatin reduced the ethanol effect on the renal corpuscular and glomerular areas and increased the urinary space area. Abbreviations: NT — non-treatment (control group); SIM5 — 5 mg simvastatin; EtOH — ethanol; EtOH + SIM5 — 5 mg simvastatin and EtOH; EtOH + SIM15 — 15 mg simvastatin and EtOH; H & E — haematoxylin and eosin staining; RC — renal corpuscle; G — glomeruli; D — distal convoluted tubule; P — proximal convoluted tubule. The same letters indicate differences between paired groups that are statistically significantly different at $P < 0.05$.

experimental groups (Fig. 1A–J). Interstitial fibrosis was scanty in the MT-stained sections of the NT or the SIM group but not in the experimental groups that were administered ethanol (EtOH, EtOH + SIM5, or EtOH + SIM15) (Fig. 2A–J). Collagen staining was most noticeable in the EtOH group (Fig. 2C, H). Likewise, the area of tissue that expressed TNF-α immunoreactivity (Fig. 3A–J) in the extracellular matrix was most conspicuous in the renal corpuscles and the renal tubules of the EtOH group (Fig. 3C and H).

Morphometry of the renal corpuscular area

In the females, the renal corpuscular area was highest in the EtOH group and lowest in the EtOH + SIM5 group (Table 2; Fig. 1K). The renal corpuscular area was significantly different across the experimental groups ($P = 0.000$). A *post hoc* test revealed that the renal corpuscular area was significantly higher in the EtOH group than in the NT group ($P = 0.001$) or the EtOH + SIM5 group ($P = 0.000$). However, the area of renal corpuscle was similar in the NT *vs.* SIM

©Polish Society for Histochemistry and Cytochemistry
Folia Histochem Cytobiol. 2024
DOI: 10.5603/fhc.95685
ISSN 0239-8508, e-ISSN 1897-5631

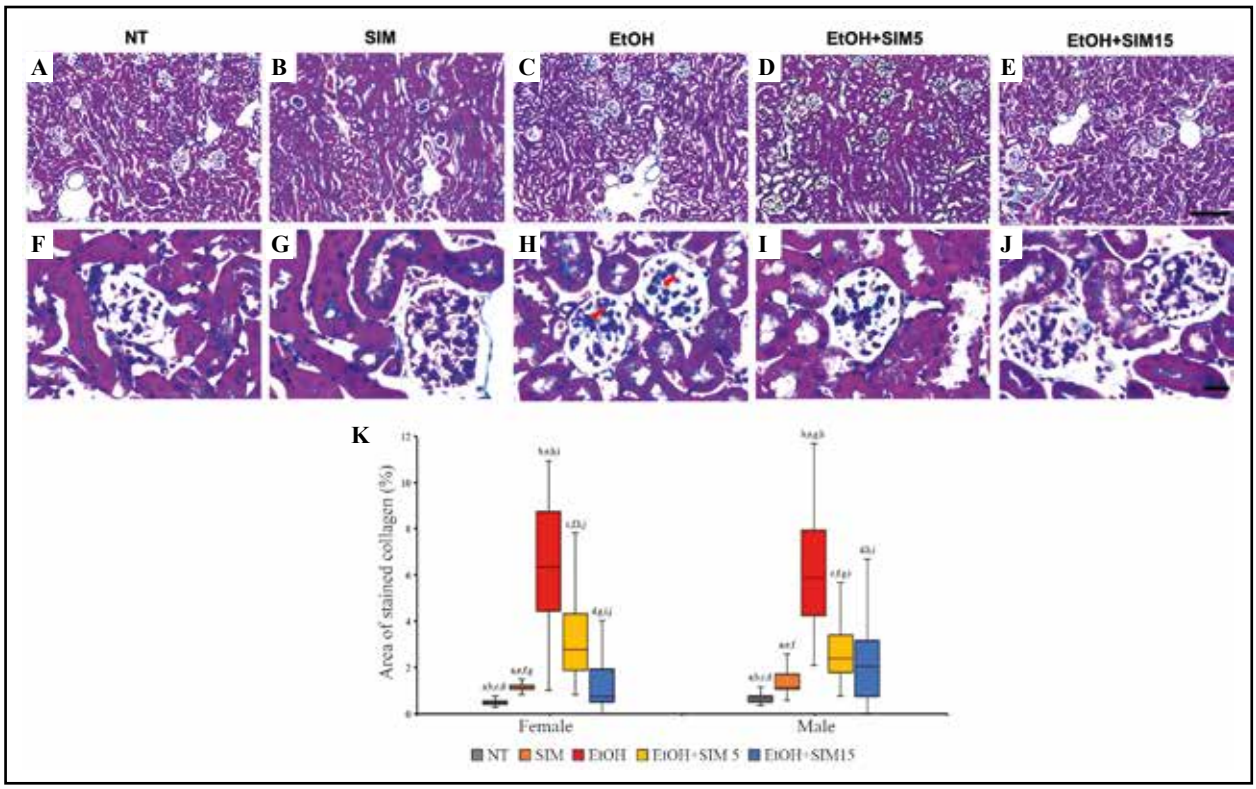

Figure 2. Representative photomicrographs of the sections of mouse kidney stained by Masson trichrome method (**A–E**) at the low magnification (scale bar: 100 μm) and (**F–J**) at the high magnification (scale bar: 20 μm) as well as the box plots of the median values of: (**k**) area of stained collagen across the different experimental groups, for both sexes. Interstitial fibrosis in the glomerulus and tubule (indicated by red arrows) was abundant in the EtOH group (C and H). In both sexes, the area of stained collagen was significantly higher in the ethanol-treated mice than in the NT groups. Both concentrations of simvastatin significantly reduced the ethanol effect on the area of stained collagen in the kidney. Abbreviations: NT — non-treatment (control group); SIM5 — 5 mg simvastatin; EtOH — ethanol; EtOH + SIM5 — 5 mg simvastatin and EtOH; EtOH + SIM15 — 15 mg simvastatin and EtOH; MT — Masson's trichrome staining. The same letters indicate differences between paired groups that are statistically significantly different at $P < 0.05$.

Table 2. The area of the renal corpuscle, the glomerular area, and the urinary space area in the kidney of female and male mice across the experimental groups

	No of animals	No of renal structures assessed	Renal corpuscular area	Glomerular area	Urinary space area
			Mean [μm^2]	Mean [μm^2]	Mean [μm^2]
Female					
NT	5	269	845 ± 381	578 ± 261	268 ± 163
SIM	5	269	858 ± 337	574 ± 231	283 ± 148
EtOH	5	268	903 ± 306	710 ± 243	193 ± 113
EtOH + SIM5	5	270	787 ± 291	545 ± 218	243 ± 122
EtOH + SIM15	5	262	881 ± 330	643 ± 241	238 ± 160
Male					
NT	5	259	857 ± 307	601 ± 236	256 ± 116
SIM	5	260	809 ± 415	529 ± 262	280 ± 185
EtOH	5	265	918 ± 288	726 ± 246	191 ± 103
EtOH + SIM5	5	269	755 ± 352	525 ± 254	230 ± 144
EtOH + SIM15	5	264	967 ± 314	755 ± 243	212 ± 144

The values express mean ± SD (standard deviation). Abbreviations: NT — non-treatment (control) groups; SIM — 5 mg simvastatin; EtOH — ethanol; EtOH + SIM5 — 5 mg simvastatin and EtOH; EtOH + SIM15 — 15 mg simvastatin and EtOH.

©Polish Society for Histochemistry and Cytochemistry
Folia Histochem Cytobiol. 2024
DOI: 10.5603/fhc.95685
ISSN 0239-8508, e-ISSN 1897-5631

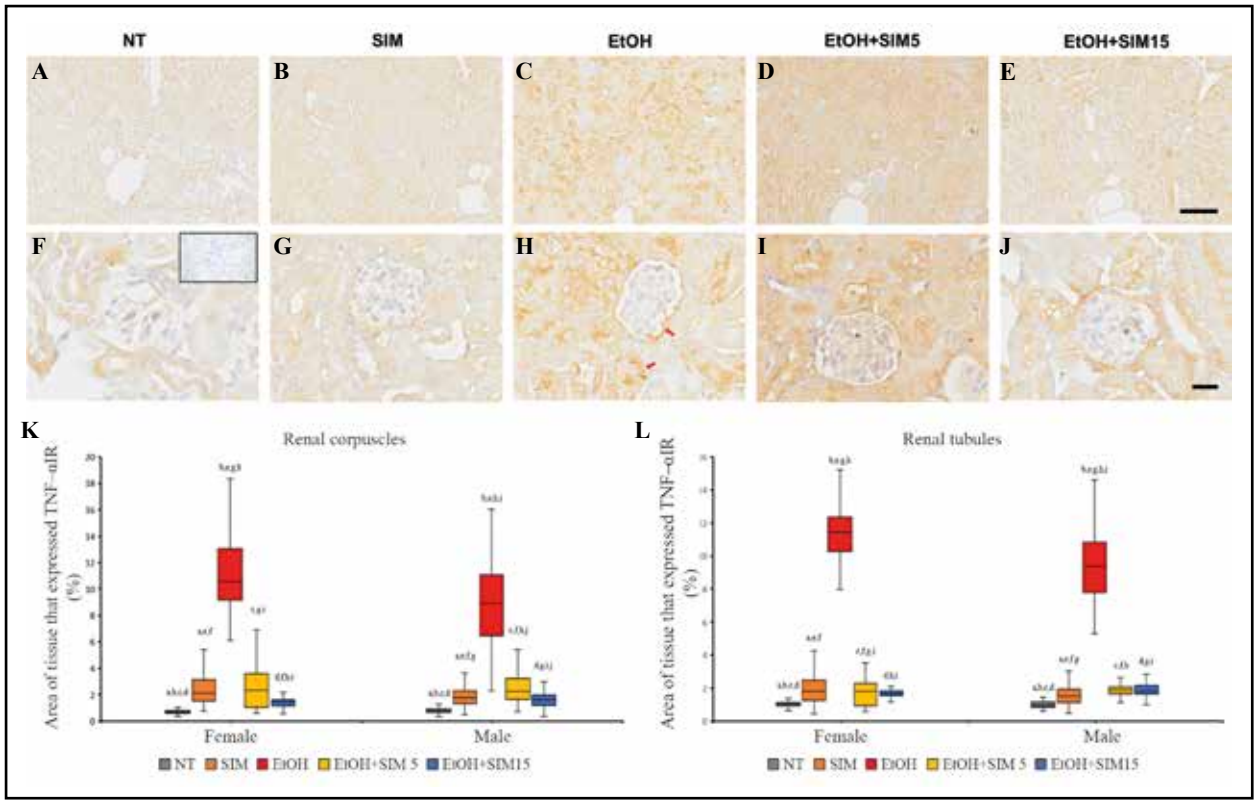

Figure 3. Representative photomicrographs of the area of mouse kidneys that expressed TNF-α IR (**A–E**) at the low magnification (scale bar: 100 μm) and (**F–J**) at the high magnification (scale bar: 20 μm) as well as the box plots of the median values of area of kidney with TNF-α IR in (a) the kidney corpuscles and (b) the kidney tubules across the different experimental groups, for both sexes. TNF-α IR in the glomeruli and the kidney tubules are indicated by the red arrows (b). The inset in (a) illustrates the reagent control where the primary antibody was omitted. In both sexes, the area of tissue that expressed TNF-α IR was significantly higher in the EtOH groups than in the NT groups in regard to the renal corpuscles and tubules. Both concentrations of simvastatin significantly reduced the ethanol effect on the area of tissue that expressed TNF-α IR in the kidney corpuscles or the tubules. Abbreviations: NT — non-treatment (control group); SIM5 — 5 mg simvastatin; EtOH — ethanol; EtOH + SIM5 — 5 mg simvastatin and EtOH; EtOH + SIM15 — 15 mg simvastatin and EtOH; TNF-α IR — Tumour Necrosis Factor-alpha immunoreactivity. The same letter indicates paired groups that are statistically significantly different at $P < 0.05$.

(P = 0.155), the NT *vs.* EtOH + SIM5 (P = 0.132), SIM *vs.* EtOH (P = 0.073) or EtOH *vs.* EtOH + SIM15 groups (P = 0.1409) (Fig. 1K). In the male mice, the renal corpuscular area was highest in the EtOH+SIM15 group and lowest in the EtOH+SIM5 group (Table 2; Fig. 1K). The renal corpuscular area was significantly different across the experimental groups (P = 0.000) and a *post hoc* test revealed that the renal corpuscular area in any paired groups was significantly different except the SIM *vs.* EtOH + SIM5 (P = 0.058) or EtOH *vs.* EtOH + SIM15 (P = 0.117) groups (Fig. 1K).

Morphometry of the glomerular area

In the female mice, the glomerular area was highest in the EtOH group and lowest in the EtOH + SIM5 group (Table 2; Fig. 1L). The glomerular area was significantly different across the experimental groups (P = 0.000) and a *post hoc* test revealed that the glomerular area in any paired groups was significantly different except the NT *vs.* SIM (P = 0.557), the NT *vs.* EtOH + SIM5 (P = 0.188), or the SIM *vs.* EtOH + SIM5 (P = 0.057) groups (Fig. 1L). In addition, the glomerular area was significantly higher in the EtOH group than in the NT (P = 0.000), SIM (P = 0.000), EtOH + SIM5 (P = 0.000) or EtOH + SIM15 groups (P = 0.001). In the male mice, the glomerular area was highest in the EtOH + SIM15 group and lowest in the EtOH + SIM5 group (Table 2, Fig. 1L). The glomerular area was significantly different across the experimental groups (P = 0.000). A *post hoc* test revealed that the area of the glomerulus in any paired groups was significantly different except for the SIM *vs.* EtOH + SIM5 (P = 0.856) or the EtOH *vs.* EtOH + SIM15 groups (P = 0.139) (Fig. 1L). In addition, the glomerular area was significantly higher in the EtOH group than in the NT (P = 0.000), SIM (P = 0.000) or EtOH + SIM5 groups (P = 0.000).

©Polish Society for Histochemistry and Cytochemistry
Folia Histochem Cytobiol. 2024
DOI: 10.5603/fhc.95685
ISSN 0239-8508, e-ISSN 1897-5631

Morphometry of the urinary space area

The urinary space area was highest in the SIM group and lowest in the EtOH group for both sexes (Table 2; Fig. 1M). In the females, the urinary space area was significantly different across the experimental groups (P = 0.000). A *post hoc* test revealed that the urinary space area was significantly lower in the EtOH group than in the NT (P = 0.000), SIM (P = 0.000), EtOH + SIM5 (P = 0.000) or EtOH + SIM15 groups (P = 0.001). However, there was no significant difference in the urinary space area in NT *vs.* SIM (P = 0.085) or NT *vs.* EtOH + SIM5 groups (P = 0.101) (Fig. 1M). In the male mice, the urinary space area was significantly different across the experimental groups (P = 0.000). A *post hoc* test revealed that the urinary space area was significantly lower in the EtOH group than in the NT (P = 0.000), SIM (P = 0.000), or EtOH + SIM5 groups (P = 0.005) but not in NT *vs.* SIM (P = 0.687) or EtOH *vs.* EtOH + SIM15 (P = 0.449) groups (Fig. 1M).

Percentage area of collagen in the kidney

The percentage area of stained collagen in the kidney was highest in the EtOH group and lowest in the NT group for both sexes (Table 3, Fig. 2K). In the female mice, the percentage area of stained collagen was significantly different across the experimental groups (P = 0.000). A *post hoc* test revealed that the percentage area of stained collagen was significantly higher in the EtOH group than in the NT (P = 0.000), SIM (P = 0.000), EtOH + SIM5 (P = 0.000), or EtOH + SIM15 groups (P = 0.000) (Fig. 2K). The significant difference between EtOH *vs.* NT demonstrates ethanol-induced collagen production in the kidney. Both concentrations of simvastatin significantly suppressed collagen production induced by ethanol, but the higher simvastatin concentration (15 mg) seems to be more effective.

In the males, the percentage area of stained collagen was significantly different across the experimental groups (P = 0.000) and a *post hoc* test revealed that the percentage area of stained collagen was significantly higher in the EtOH group than in the NT (P = 0.000), SIM (P = 0.000), EtOH + SIM5 (P = 0.000), or EtOH + SIM15 groups (P = 0.000) except in SIM *vs.* EtOH + SIM15 groups (P = 0.163) (Fig. 2K). The significant difference between the EtOH *vs.* NT groups also demonstrates ethanol-induced renal production of collagen. Similar to the females, both concentrations of simvastatin suppressed collagen production induced by ethanol in the renal tissues in the males, but the higher simvastatin concentration (15 mg) seems to be more effective.

Percentage area of tissue that expressed TNF-α immunoreactivity

The percentage area of tissue that expressed TNF-α in the renal corpuscle or the renal tubule was highest in the EtOH group and was lowest in the NT group

Table 3. The percentage area of Masson trichrome-stained collagen and the area of tissue that expressed TNF-α immunoreactivity in the kidney of female and male mice across the experimental groups

	No of animals	Area of stained collagen		Area of tissue that expressed TNF-α IR			
				Renal tubules		Renal corpuscles	
		No of images assessed	Mean [%]	No of ROIs assessed	Mean [%]	No of ROIs assessed	Mean [%]
Female							
NT	5	260	0.51 ± 0.14	205	1.03 ± 0.15	224	0.70 ± 0.15
SIM	5	260	1.48 ± 1.22	215	1.93 ± 0.84	202	2.39 ± 1.09
EtOH	5	231	6.52 ± 2.60	225	11.04 ± 1.54	252	11.13 ± 2.71
EtOH + SIM5	5	259	3.18 ± 1.73	252	1.69 ± 0.78	249	2.56 ± 1.60
EtOH + SIM15	5	257	1.35 ± 1.44	246	1.67 ± 0.20	242	1.41 ± 0.33
Male							
NT	5	260	0.67 ± 0.21	217	1.00 ± 0.21	201	0.79 ± 0.20
SIM	5	259	1.81 ± 1.66	184	1.56 ± 0.54	170	1.84 ± 0.66
EtOH	5	258	6.13 ± 5.87	248	9.51 ± 2.02	252	8.94 ± 2.92
EtOH + SIM5	5	255	2.78 ± 1.41	252	1.85 ± 0.30	252	2.48 ± 1.05
EtOH + SIM15	5	261	2.13 ± 1.49	252	1.90 ± 0.37	252	1.58 ± 0.57

The values express mean ± SD (standard deviation). Abbreviations: NT — non-treatment (control) groups; SIM — 5 mg simvastatin; EtOH — ethanol; EtOH + SIM5 — 5 mg simvastatin and ethanol; EtOH + SIM15 — 15 mg simvastatin and ethanol; ROI — Region of interest; TNF-α IR — Tumour necrosis factor-alpha immunoreactivity.

©Polish Society for Histochemistry and Cytochemistry

DOI: 10.5603/fhc.95685
ISSN 0239-8508, e-ISSN 1897-5631

for both sexes (Table 3, Fig. 3K, L). In the females, a Kruskal-Wallis test revealed that the percentage area of tissue immunoreactive for TNF-α was significantly different across the experimental groups (P = 0.000) while a Dunn's *post hoc* revealed that the percentage area of tissue that showed TNF-α immunoreactivity in any paired groups was significantly different except the SIM *vs.* EtOH + SIM5 groups (P = 0.200) for the renal corpuscles (Fig. 3K) or the SIM *vs.* EtOH + SIM15 groups (P = 0.453) for the renal tubules (Fig. 3L). The significant difference between the EtOH *vs.* NT also demonstrates ethanol-induced TNF-α production in the renal tissue and both concentrations of simvastatin reduced ethanol-induced TNF-α production in the renal tissue.

In the male mice, the percentage area of tissue that expressed TNF-α was significantly different across the experimental groups (P = 0.000) while a *post hoc* test revealed that the percentage area of TNF-α production in the renal tissue in any paired groups for the renal corpuscles or the renal tubules was significantly different except in the EtOH + SIM5 *vs.* EtOH + SIM15 groups (P = 0.733) for the renal tubule in the male (Fig. 3L). The significant difference between the EtOH *vs.* NT groups also confirms ethanol-induced TNF-α production in the renal tissue and both concentrations of simvastatin were also effective in reducing ethanol-induced inflammation in the renal tissue.

DISCUSSION

Chronic ethanol use damages renal tissues in diverse ways. It promotes the accumulation of inflammatory cells to infiltrate the interstitial tissue. Even though this is essential for triggering a repair process, prolonged accumulation of inflammatory cells and pro-inflammatory cytokines hinders the repair process which then progresses to renal disease [37, 38]. Structural renal damage such as tubular epithelial cell atrophy, renal interstitial oedema, and tubular interstitial fibrosis suppress renal function [2, 7]. Kidney tubular cell injury and apoptosis also disrupt the selective reabsorption of molecules [16, 17]. Furthermore, fluid and mineral homeostasis is also disrupted as the secretion of antidiuretic hormone (ADH) is hindered by chronic ethanol use due to the renal collecting tubules becoming impermeable to water leading to electrolyte imbalance [17, 39]. Chronic ethanol consumption results in the thickening of the glomerular basement membrane, increased proliferation of mesangial cells, and swelling of the glomeruli, thereby leading to renal dysfunction [7].

Our study revealed that prolonged ethanol administration to young adult mice enlarged the size of the glomeruli with a corresponding decrease in urinary space. These outcomes seem to be ethanol-specific because increased glomerular capillaries favour glomerular hyperfiltration with a resultant urinary space dilation owing to the high hydrostatic pressure gradient in the glomeruli. A dilated urinary space results in a reduced urinary space pressure which is expected to maintain a glomerular hyperfiltration by sustaining a high transcapillary hydrostatic pressure gradient in the glomerular capillaries [40–42]. The failure of an 'envisaged' urinary space dilation to cope with glomerular hyperfiltration may therefore lead to upstream loss of parietal epithelial cells [41] which may trigger narrowing of glomerular capillaries causing synechiae formation in glomerulosclerosis [41, 43]. According to Tobar *et al.* [41], a dilated urinary space protects against the damage that could arise from high-pressure glomerular hyperfiltration. In the present study, glomerular hypertrophy induced by ethanol reduced the size of urinary space which seems to suggest ethanol-specific renal damage. Unfortunately, the extent of the renal damage by ethanol could not be elucidated in the present study.

Ethanol is also implicated in promoting extracellular matrix build-up (*i.e.* fibrosis) in the renal interstitium surrounding the tubules and capillaries. At the early stages of renal injury, myofibroblasts are stimulated by the inflammatory cytokines to produce collagen in order to initiate a repair process [44, 45]. However, when the injury is prolonged as in the case of chronic ethanol use, a sustained accumulation of collagen damages the endothelium of capillaries and increases the distance between the capillaries and the tubules thus delaying or reducing the oxygen supply and nutrients to the epithelial tubular and interstitial cells. This invariably leads to the accumulation of collagen in the renal tissue, as found in this study, leading to kidney dysfunction [2].

Likewise, the basal concentration of TNF-α is considerably low or undetectable under normal conditions but sporadically increases at the onset of renal inflammation to trigger a recovery pathway [9, 18]. TNF-α at low levels promotes tissue repair and induces the regeneration of renal cells in order to promote recovery from injury [18]. Furthermore, TNF-α regulates renal function and controls haemodynamics through its ability to control the constriction of renal vessels, thereby affecting the rate of glomerular filtration [18]. However, this system is destabilized by the chronic use of ethanol as ethanol-induced prolonged inflammatory stress leads to structural kidney damage and dysfunction [9]. This also aligns with the observations in the present study that found that chronic ethanol significantly increased the expression

©Polish Society for Histochemistry and Cytochemistry
Folia Histochem Cytobiol. 2024
DOI: 10.5603/fhc.95685
ISSN 0239-8508, e-ISSN 1897-5631

of TNF-α in the kidney cortex, indicating ethanol-induced renal inflammation.

With the rising prevalence of ethanol use amongst adolescents, it will not be far-fetched to find that the prevalence of chronic renal diseases caused by ethanol (or other substance abuse) will also be on the rise even though there is no data available on the prevalence of ethanol-related renal diseases, specifically in this age group [46]. It is however proven that acute or chronic ethanol consumption can hinder kidney function, and this may be worsened in the presence of other metabolic diseases [17].

Simvastatin, a drug that belongs to the anti-atherosclerotic group of statins, seems to be a promising intervention for treating renal diseases as it is widely used in the treatment of cardiovascular diseases due to its ability to reduce inflammation, cell death, and fibrosis in the heart [20–23, 25, 27, 47–51]. Generally, statins inhibit the upregulation of angiotensin-dependent oxidative stress [52, 53]. More so, simvastatin inhibits the differentiation of fibroblasts into myofibroblasts thus reducing the activity of myofibroblasts and subsequently reducing collagen deposition [27]. Simvastatin is also effective in lowering blood cholesterol in subjects with chronic kidney disease [54]. Christensen *et al.* [55] reported that in mice simvastatin at a dose of 10 or 25 mg, but not 1 mg, hindered the development of glomerular hypertrophy and glomerulonephritis as a result of immune-mediated kidney damage. We are not aware of reports on the effects of simvastatin against ethanol-related renal disease. However, Mohammadi *et al.* [31] found that simvastatin reduced lead-induced renal damage in Balb/c male mice. In the same study, kidney damage was severely reduced in the mice that were treated with 20 mg simvastatin. These findings, although obtained in a different experimental model, support the results of the present study which showed that simvastatin reduced glomerular hypertrophy, renal fibrosis, and inflammation in the chronic ethanol-administration model in young adult mice. Our observations are also consistent with the findings of the simvastatin effects on ethanol-induced myocardial damage in C57BL/6J mice [56]. It is also evident in the present study that both concentrations (5 and 15 mg) of simvastatin suppressed (to varying degrees in both sexes) the onset of ethanol-induced kidney damage. Interestingly, 5 mg simvastatin was more effective for preventing the onset of ethanol-related renal damage whereas 15 mg simvastatin was more effective against ethanol-related renal fibrosis while both concentrations proved to be similarly effective against ethanol-related indices of renal inflammation. It, therefore, indicates that the effectiveness of simvastatin may be specific to the pathology (*e.g.* renal damage, fibrosis, or inflammation) induced by a toxin (*e.g.* ethanol). Additional studies are needed to further elucidate the true effects of simvastatin against ethanol-induced renal damage.

In conclusion, this study demonstrated that simvastatin suppressed the onset of ethanol-related renal damage in a murine model. Although the mechanism of action was not explored in the present study, it has been assumed that the ability of simvastatin to modulate intracellular activities may have played a vital role in preventing ethanol-induced kidney damage. Further studies on the engaged cellular pathways need to be explored. Data presented in this novel study may broaden the applications of simvastatin which could be considered for the treatment or management of ethanol-related kidney diseases.

Article information and declarations

Data availability statement

The raw data of the morphometries and analyses are available on request.

Ethics statement

Animal ethics approval was granted (Ethics Clearance No: 2019/11/63/C) by the Animal Research Ethics Committee (AREC) of the University of the Witwatersrand, Johannesburg, South Africa.

Author contributions

Conceptualization: O.I.O.; Funding acquisition: O.I.O.; Supervision: O.I.O.; Methodology: M.N., R.dP., A.E. and O.I.O.; Formal analysis: M.N. and O.I.O. Writing – original draft preparation: M.N., O.I.O. Writing – review & editing: M.N., R.dP., A.E. and O.I.O.

Funding

This work was supported by project grants of O.I.O. from the South African Medical Research Council's Self-Initiated Research Grant (SAMRC-SIR) and the National Research Foundation of South Africa (NRF TTK210301588226) Grant and by study support for M.N., A.E., and R.dP. from the National Research Foundation of South Africa (NRF).

Acknowledgments

We thank the WRAF for the animal housing and treatment and Hasiena Ali and Eric Liebenberg for technical support.

Conflict of interest

The authors declare no conflicting interests in this work.

©Polish Society for Histochemistry and Cytochemistry

DOI: 10.5603/fhc.95685
ISSN 0239-8508, e-ISSN 1897-5631

REFERENCES

1. Van Beusecum J, Inscho EW. Regulation of renal function and blood pressure control by P2 purinoceptors in the kidney. Curr Opin Pharmacol. 2015; 21: 82–88, doi: 10.1016/j.coph.2015.01.003, indexed in Pubmed: 25616035.
2. Ojeda ML, Barrero MJ, Nogales F, et al. Oxidative effects of chronic ethanol consumption on the functions of heart and kidney: folic acid supplementation. Alcohol Alcohol. 2012; 47(4): 404–412, doi: 10.1093/alcalc/ags056, indexed in Pubmed: 22596042.
3. Brzóska MM, Moniuszko-Jakoniuk J, Piłat-Marcinkiewicz B, et al. Liver and kidney function and histology in rats exposed to cadmium and ethanol. Alcohol Alcohol. 2003; 38(1): 2–10, doi: 10.1093/alcalc/agg006, indexed in Pubmed: 12554600.
4. Damman K, Testani JM. The kidney in heart failure: an update. Eur Heart J. 2015; 36(23): 1437–1444, doi: 10.1093/eurheartj/ehv010, indexed in Pubmed: 25838436.
5. Matzopoulos RG, Truen S, Bowman B, et al. The cost of harmful alcohol use in South Africa. S Afr Med J. 2014; 104(2): 127–132, doi: 10.7196/samj.7644, indexed in Pubmed: 24893544.
6. Obad A, Peeran A, Little JI, et al. Alcohol-mediated organ damages: heart and brain. Front Pharmacol. 2018; 9: 81, doi: 10.3389/fphar.2018.00081, indexed in Pubmed: 29487525.
7. Das Kumar S, Vasudevan DM. Alcohol induced effects on kidney. Indian J Clin Biochem. 2008; 23(1): 4–9, doi: 10.1007/s12291-008-0003-9, indexed in Pubmed: 23105711.
8. Hu PJ, Wu MY, Lin TC, et al. Effect of statins on renal function in chronic kidney disease patients. Sci Rep. 2018; 8(1): 16276, doi: 10.1038/s41598-018-34632-z, indexed in Pubmed: 30390007.
9. Abdollahzadeh Fa, Samadi M, Shirpoor A, et al. Ethanol consumption promotes TNF–α signaling pathway in rat kidney: rescue effect of curcumin. J Chem Health Risks. 2022; 12(2): 271–280, doi: 10.22034/jchr.2021.1913474.1211.
10. Marshall EJ. Adolescent alcohol use: risks and consequences. Alcohol Alcohol. 2014; 49(2): 160–164, doi: 10.1093/alcalc/agt180, indexed in Pubmed: 24402246.
11. Morojele N, Ramsoomar L. Addressing adolescent alcohol use in South Africa. South African Medical Journal. 2016; 106(6): 551, doi: 10.7196/samj.2016.v106i6.10944.
12. Yudhisthira NL. Renal histopathology after mixed liquor consumption in Wistar rat. GSC Biol Pharm Sci. 2022; 20(3): 324––329, doi: 10.30574/gscbps.2022.20.3.0354.
13. Swart LA, Seedat M, Nel J. Alcohol consumption in adolescent homicide victims in the city of Johannesburg, South Africa. Addiction. 2015; 110(4): 595–601, doi: 10.1111/add.12825, indexed in Pubmed: 25588696.
14. Olsson CA, Romaniuk H, Salinger J, et al. Drinking patterns of adolescents who develop alcohol use disorders: results from the Victorian Adolescent Health Cohort Study. BMJ Open. 2016; 6(2): e010455, doi: 10.1136/bmjopen-2015-010455, indexed in Pubmed: 26868948.
15. Bertscher A, London L, Rohrs SA. human rights analysis of South Africa's control of marketing of alcoholic beverages bill. Homa Publica. 2020; 4(1): 065–065.
16. Lee YJ, Cho S, Kim SR. Effect of alcohol consumption on kidney function: population-based cohort study. Sci Rep. 2021; 11(1): 2381, doi: 10.1038/s41598-021-81777-5, indexed in Pubmed: 33504820.
17. Latchoumycandane C, Nagy LE, McIntyre TM. Chronic ethanol ingestion induces oxidative kidney injury through taurine-inhibitable inflammation. Free Radic Biol Med. 2014; 69: 403–416, doi: 10.1016/j.freeradbiomed.2014.01.001, indexed in Pubmed: 24412858.
18. Kainama SY, Kakisina P, Watuguly T, et al. Expression of TNF-α on Wistar Rat (L.) with Extract of Pletekan Leaves (L.). Pak J Biol Sci. 2022; 25(10): 938–951, doi: 10.3923/pjbs.2022.938.951, indexed in Pubmed: 36404748.
19. Justo P, Lorz C, Sanz A, et al. Expression of apoptosis regulatory proteins in tubular epithelium stressed in culture or following acute renal failure. Kidney Int. 2000; 57(3): 969–981, doi: 10.1046/j.1523-1755.2000.00925.x, indexed in Pubmed: 10720950.
20. Thabit A, Alhifany A, Alsheikh R, et al. Effect of simvastatin and atorvastatin on serum vitamin d and bone mineral density in hypercholesterolemic patients: a cross-sectional study. J Osteoporos. 2014; 2014: 468397, doi: 10.1155/2014/468397, indexed in Pubmed: 25197610.
21. Liu D, Liu Y, Yi Z, et al. Simvastatin protects cardiomyocytes from doxorubicin cardiotoxicity by suppressing endoplasmic reticulum stress and activating Akt signaling. Int J Clin Exp Med. 2016; 9(2): 2193–201.
22. Morse LR, Coker J, Battaglino RA. Statins and bone health: a mini review. Actual Osteol. 2018; 14(1): 31.
23. Pedersen TR. Pleiotropic effects of statins: evidence against benefits beyond LDL-cholesterol lowering. Am J Cardiovasc Drugs. 2010; 10 Suppl 1: 10–17, doi: 10.2165/1158822-S0-000000000-00000, indexed in Pubmed: 21391729.
24. Gao K, Wang G, Wang Y, et al. Neuroprotective effect of simvastatin via inducing the autophagy on spinal cord injury in the rat model. Biomed Res Int. 2015; 2015: 260161, doi: 10.1155/2015/260161, indexed in Pubmed: 26539474.
25. Xiao X, Chang G, Liu J, et al. Simvastatin ameliorates ventricular remodeling via the TGFβ1 signaling pathway in rats following myocardial infarction. Mol Med Rep. 2016; 13(6): 5093–5101, doi: 10.3892/mmr.2016.5178, indexed in Pubmed: 27121011.
26. Bea S, Oh IS, Kim JuH, et al. High-Intensity statin reduces the risk of mortality among chronic liver disease patients with atherosclerotic cardiovascular disease: a population-based cohort study. J Am Heart Assoc. 2023; 12(8): e028310, doi: 10.1161/JAHA.122.028310, indexed in Pubmed: 37066797.
27. Cahyawati PN, Lestari D, Siskayani A, et al. Simvastatin Improves Renal Function and Glomerulosclerosis in Ischemic-reperfusion Injury. Indones Biomed J. 2020; 12(2): 143–8, doi: 10.18585/inabj.v12i2.1082.
28. Lach G, Fülling C, Bastiaanssen TFS, et al. Enduring neurobehavioral effects induced by microbiota depletion during the adolescent period. Transl Psychiatry. 2020; 10(1): 382, doi: 10.1038/s41398-020-01073-0, indexed in Pubmed: 33159036.
29. Cardoso de Sousa M, Vegian MR, Biserra MA, et al. Influence of chronic alcohol use on osteoblastic differentiation of bone marrow cells, bone properties, and hepatic and renal morphology of rats. Sci World J. 2018; 2018: 2494918, doi: 10.1155/2018/2494918, indexed in Pubmed: 30057490.
30. Patten AR, Fontaine CJ, Christie BR. A comparison of the different animal models of fetal alcohol spectrum disorders and their use in studying complex behaviors. Front Pediatr. 2014; 2: 93, doi: 10.3389/fped.2014.00093, indexed in Pubmed: 25232537.
31. Mohammadi S, Zamani E, Mohadeth Z, et al. Effects of different doses of simvastatin on lead-induced kidney damage in Balb/c male mice. Pharm Sci. 2015; 20(4): 157–162, doi: 10.5681/PS.2015.005.
32. McKay A, Leung BP, McInnes IB, et al. A novel anti-inflammatory role of simvastatin in a murine model of allergic asthma. J Immunol. 2004; 172(5): 2903–2908, doi: 10.4049/jimmunol.172.5.2903, indexed in Pubmed: 14978092.
33. Fernandes C, Marcondes S, Galindo G, et al. Kidney anatomy, histology and histometric traits associated to renosomatic index

©Polish Society for Histochemistry and Cytochemistry

in Gymnotus inaequilabiatus (Gymnotiformes: Gymnotidae). Neotrop Ichthyol. 2019; 17(4), doi: 10.1590/1982-0224-20190107.
34. Chen Y, Yu Q, Xu CBA. convenient method for quantifying collagen fibers in atherosclerotic lesions by ImageJ software. Int J Clin Exp Med. 2017; 10(10): 14904–10.
35. Latiff S, Olateju OI. Quantification and comparison of tenocyte distribution and collagen content in the commonly used autografts for anterior cruciate ligament reconstruction. Anat Cell Biol. 2022; 55(3): 304–310, doi: 10.5115/acb.22.005, indexed in Pubmed: 35668478.
36. Balzano T, Arenas YM, Dadsetan S, et al. Sustained hyperammonemia induces TNF-a IN Purkinje neurons by activating the TNFR1-NF-κB pathway. J Neuroinflammation. 2020; 17(1): 70, doi: 10.1186/s12974-020-01746-z, indexed in Pubmed: 32087723.
37. Silverstein DM. Inflammation in chronic kidney disease: role in the progression of renal and cardiovascular disease. Pediatr Nephrol. 2009; 24(8): 1445–1452, doi: 10.1007/s00467-008-1046-0, indexed in Pubmed: 19083024.
38. López-Hernández FJ, López-Novoa JM. Role of TGF-β in chronic kidney disease: an integration of tubular, glomerular and vascular effects. Cell Tissue Res. 2012; 347(1): 141–154, doi: 10.1007/s00441-011-1275-6, indexed in Pubmed: 22105921.
39. Singh VP, Singh N, Jaggi AS. A review on renal toxicity profile of common abusive drugs. Korean J Physiol Pharmacol. 2013; 17(4): 347–357, doi: 10.4196/kjpp.2013.17.4.347, indexed in Pubmed: 23946695.
40. Chagnac A, Weinstein T, Korzets A, et al. Glomerular hemodynamics in severe obesity. Am J Physiol Renal Physiol. 2000; 278(5): F817–F822, doi: 10.1152/ajprenal.2000.278.5.F817, indexed in Pubmed: 10807594.
41. Tobar A, Ori Y, Benchetrit S, et al. Proximal tubular hypertrophy and enlarged glomerular and proximal tubular urinary space in obese subjects with proteinuria. PLoS One. 2013; 8(9): e75547, doi: 10.1371/journal.pone.0075547, indexed in Pubmed: 24086563.
42. Kataoka H, Nitta K, Hoshino J. Glomerular hyperfiltration and hypertrophy: an evaluation of maximum values in pathological indicators to discriminate "diseased" from "normal". Front Med (Lausanne). 2023; 10: 1179834, doi: 10.3389/fmed.2023.1179834, indexed in Pubmed: 37521339.
43. Kuppe C, Gröne HJ, Ostendorf T, et al. Common histological patterns in glomerular epithelial cells in secondary focal segmental glomerulosclerosis. Kidney Int. 2015; 88(5): 990–998, doi: 10.1038/ki.2015.116, indexed in Pubmed: 25853334.
44. Eddy AA. Overview of the cellular and molecular basis of kidney fibrosis. Kidney Int Suppl (2011). 2014; 4(1): 2–8, doi: 10.1038/kisup.2014.2, indexed in Pubmed: 25401038.
45. Latchoumycandane C, Hanouneh M, Nagy LE, et al. Inflammatory PAF receptor signaling initiates hedgehog signaling and kidney fibrogenesis during ethanol consumption. PLoS One. 2015; 10(12): e0145691, doi: 10.1371/journal.pone.0145691, indexed in Pubmed: 26720402.
46. Steele MR, Belostotsky V, Lau KK. The dangers of substance abuse in adolescents with chronic kidney disease: a review of the literature. CANNT J. 2012; 22(1): 15–22; quiz 23, indexed in Pubmed: 22558679.
47. Patel R, Nagueh SF, Tsybouleva N, et al. Simvastatin induces regression of cardiac hypertrophy and fibrosis and improves cardiac function in a transgenic rabbit model of human hypertrophic cardiomyopathy. Circulation. 2001; 104(3): 317–324, doi: 10.1161/hc2801.094031, indexed in Pubmed: 11457751.
48. Sun F, Duan W, Zhang Yu, et al. Simvastatin alleviates cardiac fibrosis induced by infarction via up-regulation of TGF-β receptor III expression. Br J Pharmacol. 2015; 172(15): 3779–3792, doi: 10.1111/bph.13166, indexed in Pubmed: 25884615.
49. MacDougall DA, Pugh SD, Bassi HS, et al. Simvastatin promotes cardiac myocyte relaxation in association with phosphorylation of troponin I. Front Pharmacol. 2017; 8: 203, doi: 10.3389/fphar.2017.00203, indexed in Pubmed: 28469574.
50. Lee MMY, Sattar N, McMurray JJV, et al. Statins in the Prevention and Treatment of Heart Failure: a Review of the Evidence. Curr Atheroscler Rep. 2019; 21(10): 41, doi: 10.1007/s11883-019-0800-z, indexed in Pubmed: 31350612.
51. Skrzypiec-Spring M, Sapa-Wojciechowska A, Haczkiewicz-Leśniak K, et al. HMG-CoA reductase inhibitor, simvastatin is effective in decreasing degree of myocarditis by inhibiting metalloproteinases activation. Biomolecules. 2021; 11(10), doi: 10.3390/biom11101415, indexed in Pubmed: 34680049.
52. Zhou Q, Liao JK. Statins and cardiovascular diseases: from cholesterol lowering to pleiotropy. Curr Pharm Des. 2009; 15(5): 467–478, doi: 10.2174/138161209787315684, indexed in Pubmed: 19199975.
53. Zhang X, Xiang C, Zhou YH, et al. Effect of statins on cardiovascular events in patients with mild to moderate chronic kidney disease: a systematic review and meta-analysis of randomized clinical trials. BMC Cardiovasc Disord. 2014; 14: 19, doi: 10.1186/1471-2261-14-19, indexed in Pubmed: 24529196.
54. Baigent C, Landray MJ, Reith C, et al. SHARP Investigators. The effects of lowering LDL cholesterol with simvastatin plus ezetimibe in patients with chronic kidney disease (Study of Heart and Renal Protection): a randomised placebo-controlled trial. Lancet. 2011; 377(9784): 2181–2192, doi: 10.1016/S0140-6736(11)60739-3, indexed in Pubmed: 21663949.
55. Christensen M, Su AW, Snyder RW, et al. Simvastatin protection against acute immune-mediated glomerulonephritis in mice. Kidney Int. 2006; 69(3): 457–463, doi: 10.1038/sj.ki.5000086, indexed in Pubmed: 16407885.
56. Nchodu M, Efuntayo A, du Preez R, et al. Simvastatin significantly reduced alcohol-induced cardiac damage in adolescent mice. Cardiovasc Toxicol. 2024; 24(1): 15–26, doi: 10.1007/s12012-023-09821-6, indexed in Pubmed: 38261135.

Submitted: 24 May, 2024
Accepted after reviews: 24 May, 2024
Available as Online first: 19 June, 2024

©Polish Society for Histochemistry and Cytochemistry